

# UCLA

## UCLA Previously Published Works

### Title

Long-term administration of the TNF blocking drug Remicade (cV1q) to mdx mice reduces skeletal and cardiac muscle fibrosis, but negatively impacts cardiac function

### Permalink

<https://escholarship.org/uc/item/7zq85533>

### Journal

Neuromuscular Disorders, 24(7)

### ISSN

0960-8966

### Authors

Ermolova, NV  
Martinez, L  
Vetrone, SA  
[et al.](#)

### Publication Date

2014-07-01

### DOI

10.1016/j.nmd.2014.04.006

Peer reviewed

Published in final edited form as:

*Neuromuscul Disord.* 2014 July ; 24(7): 583–595. doi:10.1016/j.nmd.2014.04.006.

## Long-term administration of the TNF blocking drug Remicade (cV1q) to mdx mice reduces skeletal and cardiac muscle fibrosis, but negatively impacts cardiac function

N.E. Ermolova<sup>1,2</sup>, L. Martinez<sup>1,2</sup>, S.A. Vetrone<sup>1,2,6</sup>, M. C. Jordan<sup>3</sup>, K. .P. Roos<sup>3</sup>, H.L. Sweeney<sup>5,7</sup>, and M.J. Spencer<sup>1,2,7,\*</sup>

<sup>1</sup>Department of Neurology, David Geffen School of Medicine, University of California, Los Angeles 90095, USA

<sup>2</sup>Center for Duchenne Muscular Dystrophy at UCLA

<sup>3</sup>Department of Physiology, David Geffen School of Medicine, University of California, Los Angeles, CA 90095, USA

<sup>5</sup>Department of Physiology, University of Pennsylvania, Philadelphia, PA 19104

<sup>7</sup>Paul Wellstone Muscular Dystrophy Center

### Abstract

Duchenne muscular dystrophy (DMD) is a degenerative skeletal muscle disease caused by mutations in the gene encoding dystrophin (DYS). Tumor necrosis factor (TNF) has been implicated in the pathogenesis of DMD since short-term treatment of *mdx* mice with TNF blocking drugs proved beneficial; however, it is not clear whether long-term treatment will also improve long-term outcomes of fibrosis and cardiac health. In this investigation, short and long-term dosing studies were carried out using the TNF blocking drug Remicade and a variety of outcome measures were assessed. Here we show no demonstrable benefit to muscle strength or morphology with 10mg/kg or 20 mg/kg Remicade; however, 3mg/kg produced positive strength benefits. Remicade treatment correlated with reductions in myostatin mRNA in the heart, and concomitant reductions in cardiac and skeletal fibrosis. Surprisingly, although Remicade treated *mdx* hearts were less fibrotic, reductions in LV mass and ejection fraction were also observed, and these changes coincided with reductions in AKT phosphorylation on threonine 308. Thus, TNF blockade benefits *mdx* skeletal muscle strength and fibrosis, but negatively impacts AKT activation, leading to deleterious changes to dystrophic heart function. These studies uncover a previously unknown relationship between TNF blockade and alteration of muscle growth signaling pathways.

---

© 2014 Elsevier B.V. All rights reserved

\*Corresponding author Melissa J. Spencer 635 C. Young Dr. South, NRB Rm. 401 Los Angeles, CA 90095, USA Tel. (310) 794-5225 Fax (310) 206-1998 mspencer@mednet.ucla.edu.

<sup>6</sup>Current address: Whittier College, Department of Biology, Whittier, CA, 90608

**Publisher's Disclaimer:** This is a PDF file of an unedited manuscript that has been accepted for publication. As a service to our customers we are providing this early version of the manuscript. The manuscript will undergo copyediting, typesetting, and review of the resulting proof before it is published in its final citable form. Please note that during the production process errors may be discovered which could affect the content, and all legal disclaimers that apply to the journal pertain.

## Introduction

Muscular dystrophies are genetically inherited disorders that cause progressive, clinical muscle weakness. In Duchenne muscular dystrophy (DMD), mutations in dystrophin lead to a destabilized cell membrane followed by muscle degeneration, inflammation and regeneration. While in acute muscle injury, inflammatory cells serve an important role in phagocytosis of debris and release of growth factors that facilitate repair; the chronic inflammatory environment that results from repeated degeneration/regeneration cycles in dystrophic muscle leads to development of fibrosis, which is highly detrimental to muscle function and satellite cell mediated repair. Thus, dystrophic muscle comprises a highly dynamic environment consisting of pro-necrotic, pro-regenerative and pro-fibrotic factors that can positively or negatively modulate the outcome of the disease.

The *mdx* mouse is the genetic homologue of DMD because it possesses a mutation in the dystrophin gene, lacks dystrophin protein and its muscles undergo mild degeneration, inflammation and regeneration in a process that approximates human DMD. While human DMD muscles experience significant fibrosis, most muscles of the mouse lack significant connective tissue deposition, due to efficient repair by murine satellite cells; however, the *mdx* diaphragm fibroses to a significant degree and is often studied as a model of progressive degeneration and fibrosis in DMD. Dissecting the role of inflammation in *mdx* dystrophy is complicated by the dynamic and interconnected nature of the muscle infiltrate and the robust regenerative response[1]. Mouse studies that have assessed immune interventions have mainly examined short term outcomes and failed to examine the final phenotypic end products of muscle fibrosis and cardiotoxicity[1–3]. Since cardiomyopathy occurs in all patients with DMD, it is critical that any drugs considered for clinical trials are assessed in long-term studies to evaluate the effects of these agents on the heart.

TNF is elevated in both human[4] and mouse[5] dystrophinopathies and is a cytokine secreted by a broad variety of cells including macrophages, T cells, mast cells and fibroblasts. TNF exerts pleiotropic effects on its target tissues, depending on the local concentration and the presence of either type I or type II TNF receptors. While generally considered a pro-inflammatory cytokine, there are instances where blockade of TNF leads to a worsened disease phenotype, such as in the case of TNF blockade in multiple sclerosis (MS). Prior to clinical trials, studies had demonstrated that TNF was elevated in the EAE mouse model of MS and in humans with MS, and most showed a positive response to TNF blockade; however some divergent reports had also emerged[6–9]. In spite of the conflicting mouse data, clinical trials commenced in patients who were administered Lenercept, a recombinant TNF receptor (p55) immunoglobulin fusion protein[10], but unfortunately, the trials had to be suspended due to increased severity of symptoms. A similar set of circumstances led to failed trials of TNF blockade in patients with sepsis[11]. Thus, it is essential that studies proposing to block inflammatory mediators proceed with caution and examine long-term outcomes, due to the dynamic and interconnected nature of the inflammatory network and the potential danger of skewing the immune response towards a negative course.

Previous studies have shown that both Th1 (pro-inflammatory) and Th2 (anti-inflammatory, pro-regenerative, pro-fibrotic) type inflammatory cytokines are elevated in *mdx* muscles including the Th1 cytokines TNF, interferon gamma (IFN $\gamma$ ) and interleukin 6 (IL6) and the Th2 cytokines interleukin 10 (IL10) and transforming growth factor  $\beta$  (TGF $\beta$ ) [5]. In the muscular dystrophy literature, much focus has been placed on TNF, due to the availability of TNF blocking drugs and their success in reducing the severity of several inflammatory diseases such as inflammatory bowel disease and rheumatoid arthritis. Several FDA approved, TNF blocking drugs are available including Enbrel® (etanercept), Remicade® (infliximab) and Humira® (adalimumab) and are in widespread use for a variety of diseases. Early investigations of TNF blockade in the *mdx* mouse were somewhat conflicting, but primarily supported TNF blockade as beneficial for the phenotype. While ablation of TNF in the *mdx* mouse was not advantageous in short-term studies [12], long term investigation of pulmonary function showed promise [13]. Subsequent studies examining the efficacy of TNF blocking drugs Remicade (Cv1q) [2, 14, 15] or Enbrel [3, 16] on early features of *mdx* dystrophy also reported reduced necrosis and improved exercise fatigue, but also demonstrated that TNF blockade interfered with muscle repair [14]. The latter finding is consistent with the documented role of TNF in myogenesis and post-natal muscle repair [17]. TNF has been shown to play both positive and negative roles on muscle mass and myogenesis. On the one hand, high levels of TNF can induce cachexia [18–20], but on the other hand, TNF can promote muscle regeneration [17]. Since regenerated dystrophin deficient fibers are more stable than mature dystrophin deficient fibers, they significantly slow the course of the dystrophic process; thus, the effect of any pharmacological intervention for Duchenne on muscle repair is important to evaluate.

In this investigation, we examined the effect of TNF blockade on muscular dystrophy pathogenesis with a particular focus on the long-term outcomes of fibrosis and cardiomyopathy. Furthermore, we employed both traditional methods of quantitative histology and biochemistry in parallel with non-invasive methods, such as functional strength testing and imaging, to obtain a robust assessment of the phenotype. We show that higher dosing of Remicade (10 and 20 mg/kg) does not confer benefit on either muscle strength or fibrosis, but that long-term administration of low dose Remicade is beneficial for both muscle strength and fibrosis. However, improvements in skeletal muscle strength coincide with reduced cardiac function and alterations in cardiac AKT signaling. These studies call into question the potential utility of TNF blocking drugs for treatment of DMD, and suggest that commencement of trials proceed with great caution and attention to cardio toxic side effects.

## MATERIALS AND METHODS

### Animals

*mdx*(C57BL/10ScSn-*mdx*/J) breeder mice were obtained from the Jackson Laboratories and housed and bred in the UCLA vivarium in compliance with the regulations of the Department of Laboratory and Animal Medicine. All experimental protocols and use of animals were conducted in accordance with the National Institute of Health Guide for Care

and Use of Laboratory Animals and approved by the UCLA Institutional Animal Care and Use Committee.

### Injection regimen

Four different treatment regimens, that varied by the age of the mice, drug concentration and duration of treatment, were utilized in the current study (Table 1). The regimens were as follows: (1) Remicade injected i.p. (10 mg/kg of body weight) for 6 weeks starting at 2 weeks of age (treatment from 2–8 wks of age). The control group consisted of mice injected with a control antibody provided by Centocor. This experiment included 5 *mdx* controls and 6 Remicade treated animals; (2) Remicade (10 mg/kg of body weight) injected i.p., once weekly for 7 weeks starting at 28 weeks of age (treatment from 28–36 wks of age). This experiment had 9 control *mdx* mice and 10 Remicade treated *mdx* mice; (3) Remicade (20 mg/kg of body weight), injected once weekly, i.p., for 32 weeks starting at 3 weeks of age (treatment from 3–36 wks of age). This experiment had 4 control *mdx* mice and 5 Remicade treated *mdx* mice; (4) Remicade (3 mg/kg of body weight) injected i.p. once weekly and Enbrel (4 mg/kg of body weight) injected i.p. once weekly for 24 weeks, starting at 6 weeks of age (6–30 wks of age). The control group consisted of 7 *mdx* mice, Remicade group consisted of 9 *mdx* mice and Enbrel treated group consisted of 8 *mdx* mice.

### Wire test

This test gives an approximation of whole body strength. For the wire hang test, the mouse was placed on a suspended wire that was 2 ft from the floor. Mice were allowed to hang from a wire using only their forelimbs and hind limbs. Each mouse was subjected to 5 trials with one minute of rest between trials. Hang time was recorded from the moment the experimenter gently released the mouse onto the wire until the mouse fell on the safety net. The latency to fall off the wire in seconds was scored in five trials. The mean hang time from each mouse was used for statistical analysis.

### Rotor-Rod

A Rotor-rod apparatus (San Diego Instruments, San Diego, CA) was used to assess motor performance. Mice were placed on a rotating rod in a box equipped with a laser beam to record when the mouse fell off. The rod was initially accelerated from 2.5 to 10 rpm over a period of 90 seconds. Subsequently, the speed was accelerated by 2.5 rpm every 30 seconds. Latency to fall was recorded for each trial. Each mouse performed 5 trials and was allowed to rest 1 minute between trials. The last three trials were used to calculate average latency to fall for statistical analysis.

### Grip strength

Forelimb grip strength was measured using a digital force gauge (DFIS 2, Chatillon CE). In each trial, the mouse was allowed to grasp a metal rod and the technician slowly pulled the mouse by the tail until the digital gauge recorded the peak tension produced (in Newtons). Five trials were performed with a minimum of 30-seconds rest in between. Upon completion of the grip strength test, the body weight was recorded. Average peak tension produced in all 5 trials was normalized for body weight.

### Run to exhaustion

For experiments 1 and 2, mice were given a “run to exhaustion” test. The day prior to harvesting muscles, mice were run to exhaustion, using a horizontal Eco 3/6 treadmill (Columbus Instruments, Columbus Ohio). Mice were initially run at a speed of 10 m/min (for 5 min) and then the speed was gradually increased to 16 m/min for one hour of running. Subsequently, the speed was increased to 19 m/m and was increased 1 m/min every 5 minutes (to a maximum of 25 m/min) until 1 hour and 30 minutes. Thereafter the speed was increased 1 m/min every minute up to 30 m/min. The mice were constantly monitored while running, to make sure they stayed on the treadmill and did not fall on the electrical stimulating grid. Exhaustion measurement was based on the 3-strike rule. A strike is marked when the mouse fell on the electrical grid. Once a mouse hit 3 strikes, the time was recorded.

### Echocardiography

To access cardiac function, mice underwent echocardiography analysis using a two-dimensional, M-mode and Spectral Doppler analysis, as previously described[21]. Images were acquired by a Siemens Acuson Sequoia C256 equipped with a 15L8 15-MHz probe (Siemens Medical Solutions, Mountain View, CA). Mice were anesthetized with 1% isoflurane and heart rates were maintained between 450 and 600 beats per minute during the procedure. Data were analyzed using the Acuson and AccessPoint software (Freeland Systems LLC, Santa Fe, NM, USA).

### Magnetic resonance imaging

MRI technique was performed on a horizontal bore Bruker 7.0T MRI scanner. Animals, anaesthetized with a constant supply of 2.5% isoflurane in 0.25–0.3% oxygen flow, were positioned in a non-magnetic plastic holder that supported a custom-built coil placed above the outstretched left hind limb of the animal. Their respiratory rate and body temperature were constantly monitored during the experiment. Coronal and sagittal  $T_1$  weighted spin echo images were acquired in order to determine optimal slice location for T2 measurements. T2-weighted spin-echoes (NE=6) of the left hind limb from each mouse were collected, each with a matrix size of 192×192 (field of view = 3.5 × 3.5 cm). Slice thickness was 1 mm. The echo times were 10.00, 20.00, 30.00, 40.00, 50.00, 60.00 ms. Total examination time did not exceed 40 min. Images were segmented using image-processing software (MyPav and ImageJ). T2-maps were calculated based on single spin echo images (TE=10 and 50 ms). Quantification of areas by pixel counting and differences in signal contrast within the dystrophic lesion areas were done to evaluate efficacy of treatment. Measurements were normalized to total area of limb.

### Real-time RT-PCR

Real time, RT-PCR was performed as described earlier (Vetrone, 2009). Briefly, total RNA was isolated from muscles of treated animals using Trizol reagent (Invitrogen) according to the manufacturer's protocol. Genomic DNA contamination was removed by DNase treatment for 30 min at 37°C. To produce cDNA, 2 µg of DNA-free RNA was used for first-strand cDNA synthesis with random hexamer primers and Superscript III reverse

transcriptase (Invitrogen). The resulting cDNAs were used for PCR amplification using the following primers:

iNOS (124 bp; annealing T=60.5°C):

sense 5'- CTGCAGCACTTGGATCAG-3';

antisense 5'-CGTACCAGGCCCAATGAG-3'.

Osteopontin (150 bp; annealing T=60.5°C):

sense 5'- GATGATGATGACGATGGAGACC-3';

antisense 5'-CGACTGTAGGGACGATTGGAG-3'.

TGF-beta (147 bp; annealing T=63.8°C):

sense 5'-GGGAAGCAGTGCCCGAACCC-3';

antisense 5'-TGGGGGTCAGCAGCCGGTTA-3'.

IL-6 (154 bp; annealing T=63.8°C):

sense 5'- GAACAACGATGATGCACTTGC-3';

antisense 5'-CTTCATGTACTCCAGGTAGCTATGGT-3'.

IGFBP3 (133 bp; annealing T=52°C):

sense 5'-CAGGCAGCCTAAGCACCTAC-3';

antisense 5'-AACTTGAATCGGTCACCTCG-3'.

IGFBP4 (211 bp; annealing T=52°C):

sense 5'-TTGATGCACGGGCAAGGCGT-3';

antisense 5'-CGGGGTTCTCCCGAGGTGT-3'.

IGFBP5 (136 bp; annealing T=52°C):

sense 5'-TGCACCTGAGATGAGACAGG-3';

antisense 5'-GAATCCTTTGCGGTCACAGT-3'.

Myostatin (104 bp; annealing T=52°C):

sense 5'-CTGTAACCTTCCCAGGACCA-3';

antisense 5'-GCAGTCAAGCCCAAAGTCTC-3'.

Collagen 1A1 (131 bp; annealing T=60°C):

sense 5'- GTCGCTTACCTACAGCAC -3';

antisense 5'- CAATGTCCAAGGGAGCCAC -3'.

Parallel reactions were run with the same cDNA samples and GAPDH-specific primers:

sense 5'-TCCACCACCCTGTTGCTGTA-3';

antisense 5'-GACTTCAACAGCAACTCCCAC-3' (125 bp).

PCR amplification using these primers resulted in the generation of single bands as demonstrated by conventional PCR (data not shown). All real-time reactions were performed using IQ™ SYBR Green Supermix PCR reagent (Bio-Rad) and MyIQ™ Single Color Real-time PCR Detection System (Bio-Rad). Optical System Software Version 1.0 (Bio-Rad) was used to analyze the results. Quantification utilized standard curves made from serial dilutions of control cDNA sample. Data from each sample were normalized by dividing the quantity of target gene cDNA by the quantity of housekeeping gene cDNA (GAPDH) to correct for variability in the individual samples.

### Evaluation of collagen content

Collagen content was evaluated by two independent methods, Sircol Soluble Collagen Assay Kit (Accurate Scientific) and Hydroxyproline assay. For the Sircol assay, diaphragms were homogenized in 7 volumes of Complete Buffer (Roche), sonicated for 30 seconds and centrifuged at 10,000 g for 10 minutes. Supernatants were passed through a 1.2 µm filter. After 50 µl of each sample was mixed with equal volume of 0.5 M acetic acid, 1.0 ml of Sircol Dye Reagent was added and mixed for 30 min at room temperature. After subsequent centrifugation at 10,000 g for 10 minutes the supernatant was discarded and 1.0 ml Sircol Alkali Reagent was added to the tube. Afterwards 100 µl of each sample was transferred to a 96-well ELISA plate and absorbance was recorded at 540 nm by a MultiSkán plate reader (Thermo Fisher Scientific). Data were normalized by total solubilized protein. Hydroxyproline content was performed by an independent outsourced facility (AAA Laboratories). Data were normalized for wet weight of the muscle tissue.

Collagen content in the hearts of *mdx* mice treated with Remicade and Enbrel was also estimated by staining a series of frozen sections from each treated animal with rabbit anti-collagen I antibody 1:500 (Cedarlane). This method was used due to limited availability of cardiac tissue. Secondary staining was carried out with Anti-rabbit-biotin 1:200, Avidin D-HRP 1:1000. The AEC peroxidase substrate kit from Vector Laboratories was used to visualize specific staining. Subsequently slides were placed in an automated scanning system (ScanScope AT) and quantitation was analyzed by Definiens software. Collagen content in the hearts of treated and untreated animals was expressed as the percentage of collagen I content in the total cross sectional area.

### Creatine kinase activity

Blood samples were collected by retro-orbital puncture using heparinized capillary tubes and collected in serum separating tubes. Samples were microcentrifuged at 2,200 g for 5 minutes and serum was removed and frozen at -80°C. The assay was performed using the Creatine Kinase-SL Kit from Genzyme Diagnostics (Charlottetown, Canada) according to manufacturer's instructions. A Synergy HT multi-detection microplate reader (Biotek Instruments, Winooski, VT) was used to read absorbance at 340nm.

### Muscle histology and immunohistochemistry

Muscles were dissected from the mice, placed in O.C.T. Compound (Sakura Finetek, Torrance, CA, USA) and frozen in isopentane cooled in liquid nitrogen. Frozen sections were cut at 10 µm and kept frozen until use. Immunohistochemistry was carried out with the



following antibodies and dilutions; rat anti-CD11b (Abcam, 1:50), rabbit anti-collagen 1:500 (Cedarlane), mouse anti-dMHC 1:25 (Novocastra), rat anti-CD68 1:50 (AbDSerotec). All images were acquired using an Axio Imager M1 microscope with software.

### Sample preparation and immunoblotting

Frozen skeletal or cardiac muscle tissues were homogenized on ice in 30 volumes (w/v) of reducing sample buffer [80 mM Tris-HCl (pH 6.8), 2% (w/v) sodium dodecyl sulfate, 10% (v/v) glycerol, 100 mM dithiothreitol], containing 2× Halt Protease/Phosphatase Inhibitor Cocktail (Thermo Scientific), boiled for 2 min and then centrifuged at 10 000g for 5 min at 4°C. Equal amounts of protein (100 µg) were separated by SDS-PAGE and transferred to a nitrocellulose membrane (100 V, 1 h, 4°C). Membranes were probed with the following antibodies: rabbit anti-Akt, anti-phospho-Akt (Thr308) and anti-phospho-Akt (Ser473) 1:1000 (Cell Signaling); rabbit anti-phospho-p70S6 1:1000 (Cell Signaling); mouse anti-phospho-pGSK (Tyr279/Tyr216) 1:500 (Upstate); mouse anti-CAMKII 1:500 (Invitrogen), mouse anti-phospho-CAMKII (Thr286) 1:1000 (Thermo Scientific). Anti-mouse and anti-rabbit IgG peroxidase conjugates were from Sigma-Aldrich. Blots were developed using ChemiGlow West substrate (ProteinSimple).

### Statistical analysis

Statistical analysis of all data was carried out by Student's *t*-test. Differences were considered statistically significant if the *p*-value was <0.05. Error bars on all graphs are represented by standard errors of means (SEM).

## RESULTS

### Short-term treatment of either young or old mdx mice with 10mg/kg Remicade (CV1q) does not result in obvious histological or strength benefits

Short-term treatment with Remicade (10mg/kg or 20 mg/kg administered once weekly) was previously shown to improve strength and reduce necrosis of *mdx* muscles[2, 3]. We sought to replicate those earlier results, prior to carrying out long-term treatment studies with this drug. Injections of 10mg/kg Remicade were initiated in male *mdx* mice at either 2 weeks or 30 weeks of age and mice were dosed for 6 weeks total (2–8 weeks vs 28–36 weeks of age). Mice were exercised on a treadmill for the last three weeks of the treatment period. Mice were subjected to a final run to exhaustion at the end of treatment, because prior studies showed TNF blockade improved exercise endurance[14]. After 6 weeks of treatment, mice were assessed for histological and phenotypic changes. This analysis did not reveal differences in body weight at either time point following two weeks of treatment, nor were there differences in skeletal muscle (quadriceps, tibialis anterior, gastrocnemius, hamstrings, triceps, diaphragm) or heart weight at either time point (Suppl. Fig. 1). Functional tests of muscle strength were carried out. Neither the wire test (Fig. 1A) nor the Rotor-rod (Fig. 1B) demonstrated functional improvement in the treated mice.

Histological assessment of both necrotic and regenerative areas was carried out on cross sections from treated and control mice in both the young and old groups. To assess necrosis and inflammation, slides were stained with CD11b and all pathological areas were

quantified on two cross sections per animal and values were normalized by cross sectional area as previously described [1]. To assess regeneration, slides were stained for developmental myosin heavy chain, which is only expressed in regenerating fibers, and the value normalized for total number of fibers in a cross section. No significant difference in the percent of the cross sectional area occupied by pathological or regenerative tissue was observed after 6 weeks of 10 mg/kg Remicade treatment in either young or old mice (Fig. 1C,D). Thus, short-term treatment with Remicade at 10 mg/kg does not provide obvious benefit to *mdx* pathology or strength. In addition, this dosage and duration of Remicade does not appear to impair regeneration in vivo.

### **Long-term treatment with Remicade (Cv1q) 20mg/kg does not result in phenotypic improvements**

The efficacy of a higher dosage of Remicade (20 mg/kg) was also tested in *mdx* mice in this study, because it was previously demonstrated that 5 day or 9 day treatment of *mdx* mice at this dosage resulted in impaired regeneration and increased necrosis[14]. In the prior study 90 day treatment appeared to benefit exercise tolerance and led to reduced CK[14]. Since any DMD treatment would be implemented over long periods of time, we dosed the animals weekly for 32 weeks (from 3 to 36 weeks of age) with 20mg/kg, and tested the effect on the *mdx* phenotype. Treated mice were exercised for the last 4 weeks of the treatment period using uphill exercise on a treadmill, two times a week for 30 min at 19 m/min. At the end of the exercise and treatment period, several non-invasive functional and imaging studies were conducted. No improvement in either grip strength or wire tests was observed following this treatment regimen (Fig. 2A). Creatine kinase was also unchanged after treatment (Fig. 2B). Furthermore, total collagen content was unchanged in the diaphragm (data not shown). Thus, this dosage of Remicade did not demonstrate improvements in strength or fibrosis after long-term treatment.

Magnetic resonance imaging was carried out on a subset of treated mice to determine if global changes in muscle integrity and health could be detected following 20mg/kg Remicade treatment. T2 maps were generated on the quadriceps muscles of treated and control mice, and the average voxel intensity of the signal was compared between groups. No difference in signal intensity was observed (Fig. 2C).

Echocardiography was carried out to assess the long-term consequences of 20 mg/kg Remicade treatment. Following treatment, there was no obvious decrement in cardiac function; however, a significant reduction in left ventricular mass was observed (Supp. Fig. 2). Thus 20mg/kg Remicade treatment does not result in measurable deficits in cardiac function, although this dosing might impact compensatory cardiac hypertrophy.

### **Long term treatment with low dose Remicade (3 mg/kg), but not Enbrel (4 mg/kg), results in improved strength**

A much lower dosage of Remicade was also tested (3mg/kg) and a second TNF blocking drug called Enbrel (Etanercept, 4mg/kg) was tested in parallel in long term experiments. Previous studies demonstrated histological improvements in necrosis, and reductions in CK following a short-term treatment regimen of Enbrel 4 mg/kg in *mdx* mice [3]. We sought to

test the long-term efficacy of this dosing and to examine its effect on phenotypic features of cardiomyopathy and fibrosis in the *mdx* mouse. Once weekly treatments of both drugs were initiated at 6 weeks of age and continued until the mice were 30 weeks of age. Mice were exercised two times a week for 30 minutes at escalating speeds of 10, 12 and 14 m/min. on a treadmill using a 7-degree uphill incline. Exercise was initiated when the mice were 21 weeks of age and was continued until they were 30 weeks of age.

Functional tests revealed that this dosing of Enbrel was not beneficial for increasing strength assessed by either grip strength (Fig. 3A) or wire test (Fig. 3B); however, this lower dosing of Remicade benefitted strength in both tests. Remicade treated mice performed significantly better on both the grip strength and wire tests. Neither group showed improvements in the Rotor rod, nor the treadmill endurance test (Fig. 3C and 3D).

The quadriceps muscles were examined by magnetic resonance imaging (MRI) without contrast, for signs of necrosis/inflammation (Supp. Fig. 3). The MRI signal, (representing damaged/inflamed areas), was quantitated whereby both the signal intensity (normalized to muscle volume) and the average voxel intensity was assessed. Neither measurement demonstrated improvements following drug treatment.

### **Long term treatment with Remicade 3mg/kg and Enbrel 4mg/kg results in reduced diaphragm and cardiac fibrosis**

Muscle fibrosis is a long-term consequence of the dystrophic process, which causes significant stiffness, contractures and debilitation in patients with dystrophinopathy. Since TNF is known to promote fibrosis indirectly through its effects on inflammation and downstream levels of TGFbeta, we assessed fibrosis in the diaphragms of *mdx* mice treated for 24 weeks with Remicade or Enbrel. Collagen content was assessed by both hydroxyproline and Sircol collagen assay. Both tests revealed a significant reduction in collagen content following long-term treatment with either 3 mg/kg Remicade or 4 mg/kg Enbrel (Fig. 4). Collagen I mRNA content was assessed by real time, quantitative PCR of diaphragm and heart muscles. Although a trend towards a reduction was observed in diaphragm and heart, no statistically significant difference in collagen mRNA was detected following treatment.

Histopathological assessment of skeletal and cardiac muscles was carried out to investigate whether the biochemical reductions in collagen translated to obvious morphological changes following treatment with Remicade or Enbrel. Cross sections of diaphragm muscles were stained with antibodies against collagen type I and CD68 (an M1 macrophage marker), as well as hematoxylin and von Kossa stains. These assessments did not reveal any obvious changes in fibrosis, histopathology or regeneration, since muscles in all groups were indistinguishable (Figs. 5, 6 and Supp Fig. 4). Heart muscle cross sections stained with collagen 1a were quantitatively assessed using an unbiased slide scanner (Fig. 6). This analysis revealed a significant reduction in cardiac collagen I content, supporting biochemical findings that TNF blockade reduces fibrosis. Thus, although the histological differences were not obvious, quantitative assessment revealed a reduction in collagen I deposition I both skeletal and cardiac muscles.

### TNF blockade impacts myostatin mRNA concentration

To gain insight into mechanisms responsible for Remicade's improvement of the *mdx* phenotype, assessment of several inflammatory cytokines and signaling pathways was undertaken. Several inflammatory mediators were assessed by quantitative real time PCR in the diaphragm including iNOS, a marker of M1 macrophages, and osteopontin, which is a cytokine that is highly increased in dystrophic muscles. In addition, IL-6 (an anti-inflammatory myokine) and TGF-beta (an anti-inflammatory and pro-fibrotic cytokine) were assessed. No changes were observed in the expression of any of these markers by qPCR. (Supp. Fig. 5).

Growth signaling pathways were also investigated in skeletal and cardiac muscles of treated mice, including NF $\kappa$ B, JNK and CaMK (data not shown and supplemental data Fig. 8). TGF $\beta$  family member myostatin was assayed, due to its' role as a negative regulator of muscle growth and promoter of fibrosis.[22, 23] Quantitative real time PCR revealed significant reductions in myostatin mRNA in the heart of Remicade treated animals, and a trend towards reduction, but no significant difference in myostatin mRNA in skeletal muscle. The known association between myostatin and promotion of collagen deposition suggests that reductions in fibrosis may be due to decreases in myostatin in the heart (Figure 7). Muscle volume (by MRI) or muscle mass (by weight) did not increase in Remicade treated mice (Supp. Fig. 3). Thus, the reduction in cardiac fibrosis obtained by Remicade treatment may be partially attributable to reductions in myostatin expression.

### Long-term treatment with Remicade 3mg/kg is cardiotoxic, due to reductions in LV mass

Mice subjected to long-term treatment with Remicade (20mg/kg for 32 weeks or 3mg/kg for 24 weeks) and Enbrel (4mg/kg) were also subjected to echocardiography to determine the effect of treatment on cardiac function (Fig. 8 and Supp. Fig. 2). This analysis revealed a correlation between significantly worsened cardiac function and low dose Remicade treatment. Left ventricular mass was reduced following long-term treatment with 3 mg/kg or 20 mg/kg Remicade (Fig. 8 and Supp Fig. 2) and the 3 mg/kg dose led to reductions in left ventricular ejection fraction and reduced fractional shortening. Thus, low dose Remicade appears to benefit skeletal muscle strength and skeletal and cardiac fibrosis, but this dose adversely impairs cardiac muscle growth and function.

### TNF blockade reduces AKT phosphorylation on Thr308

We sought to identify other pathways by which cardiac growth might be impacted. Both calcium calmodulin kinase (CaMK) signaling and AKT signaling have been associated with cardiac hypertrophy and were therefore assayed in hearts from treated animals [24–26]. While CaMK signaling was not significantly reduced by Remicade or Enbrel treatment (Supp. Fig. 8), a significant decrease in AKT phosphorylation on Thr308 was observed in Remicade treated mice. On the contrary, phosphorylation of AKT on Ser473 was not altered by Remicade treatment (Figure 9). Phosphorylation on Thr308, is known to be “mitogen dependent”, induced by growth factors and carried out by a downstream cellular kinase, while phosphorylation on Ser473, is attained by autophosphorylation; thus, these data suggest that Remicade interferes with growth factor dependent AKT signaling[27].

The decrease in AKT activation might be explained by increases in IGF binding proteins (IGFBP), which would effectively decrease the availability of IGF. Assessment of IGFBP mRNA by quantitative RT PCR revealed a significant decrease in IGFBP4. Decreased IGFBP would be expected to increase IGF levels and have the opposite impact on AKT signaling than that observed (supplemental Figure 7); thus, the reduction in mitogen-activated AKT phosphorylation is not explained by changes in IGFBPs.

## Discussion

Duchenne muscular dystrophy results from mutations in the gene encoding dystrophin (DYS), a cytoskeletal protein that resides on the inner surface of the sarcolemmal membrane. Dystrophin links cytoskeletal actin to the dystrophin glycoprotein complex (DGC)[28, 29]. In the absence of dystrophin, the entire DGC complex is lost and plasma membrane integrity is compromised[30]. While muscle regeneration by satellite cells can help counter the degeneration, it does not completely compensate for the persistent muscle damage, which leads to a gradual loss of muscle cells. Repeated cycles of muscle membrane rupture lead to accumulation of a complex mixture of both Th1 and Th2 inflammatory mediators, both of which have the potential to influence dystrophic pathophysiology in a variety of ways[5]. Over time, the milieu becomes skewed towards Th2-type mediators, leading to accumulation of TGFbeta and other pro-fibrotic molecules that induce remodeling and fibrotic tissue deposition[31, 32].

In the current study, we examined the consequence of long term pharmacological targeting of TNF on the *mdx* phenotype. Several different dosage regimens were employed, but only one proved efficacious in reducing deleterious features of the disease. Remicade treatment at 3 mg/kg significantly increased skeletal muscle strength and decreased both cardiac and skeletal fibrosis; however, this dosage significantly reduced cardiac muscle compensatory hypertrophy and resulted in reduced cardiac function. Interestingly, this dosage is lower than the lowest FDA recommended dose in human patients for diseases such as Crohn's disease and Colitis (5 mg/kg). Furthermore, while Remicade is counter-indicated for patients with heart disease, adverse events have only been observed in the highest dosage of 10 mg/kg. The explanation for why the lowest dosage of Remicade induced adverse changes in the dystrophic heart is not clear.

Three downstream pathways are activated in response to binding of TNF homotrimers to type I or type II TNF receptors (TNF R1 or TNF R2). While most cells express TNF R1, TNF R2 is mainly expressed on immune and endothelial cells. Downstream signaling from TNF receptors can activate diverse signaling pathways that include NFKB, MAPK, AKT and caspase that trigger either cell death or cell survival, depending on a variety of factors[33, 34]. Activation of TNF R1 tends towards induction of apoptosis whereas activation of TNF R2 tends towards activation of NFKB and cell survival. [35] TNF signaling has not been previously linked to myostatin signaling.

In this study, low dose Remicade treatment correlated with reductions in myostatin mRNA in the heart, and decreased cardiac muscle fibrosis. These studies reveal a previously unknown benefit of Remicade treatment of reducing myostatin expression in the heart.

However, although lower myostatin levels are normally associated with increased muscle growth; no increase in cardiac muscle mass or volume was observed in Remicade treated mice, likely due to the concomitant reductions in AKT activation. AKT and myostatin signaling pathways exert opposing outcomes on muscle growth [36, 37], and the dystrophic phenotype [38–40]. Myostatin signaling impairs muscle growth, whereas AKT signaling stimulates hypertrophy. In this study, both pathways were reduced following Remicade treatment at 3mg/kg. Thus, one conclusion that could be drawn from these data is that the beneficial affect of reduced cardiac fibrosis was attributable to lowered myostatin, but this improvement did not translate to enhanced cardiac function, due to concomitant reductions in cardiac AKT signaling.

The investigation here demonstrates benefit to skeletal muscle from low dose Remicade treatment. This improvement appears to be attributable to reduced skeletal muscle fibrosis. Unfortunately, the observed, concomitant reductions in AKT signaling have a negative impact on cardiac growth. While caution is urged when extrapolating from the mouse to human disease, these studies suggest that trials of Remicade in DMD patients proceed with extreme care and extensive cardiac surveillance. Additional studies will be necessary to gain insight into specific mechanisms involved in these signaling changes.

## Supplementary Material

Refer to Web version on PubMed Central for supplementary material.

## Acknowledgments

This work was supported by funding from the National Institute of Arthritis, Musculoskeletal and Skin Diseases for a Wellstone Cooperative Muscular Dystrophy Center (U54AR052646-Sweeney) and a P30 Muscular Dystrophy Core Center (P30AR057230-01-Spencer). Funding was also provided by Parent Project Muscular Dystrophy (Spencer) and the Muscular Dystrophy Association (Spencer). Mouse specific Remicade (infliximab) was generously supplied by Centocor. Mouse specific Enbrel (etanercept) was generously supplied by Amgen. Cardiac assessment was carried out by the UCLA Mouse Heart Physiology Core. All other functional assessments were carried out in the Center for Duchenne Muscular Dystrophy Mouse Phenotyping and Imaging Core.

## References

1. Spencer MJ, Montecino-Rodriguez E, Dorshkind K, Tidball JG. Helper (CD4(+)) and cytotoxic (CD8(+)) T cells promote the pathology of dystrophin-deficient muscle. *Clin Immunol.* 2001; 98:235–243. [PubMed: 11161980]
2. Grounds MD, Torrisi J. Anti-TNFalpha (Remicade) therapy protects dystrophic skeletal muscle from necrosis. *Faseb J.* 2004; 18:676–682. [PubMed: 15054089]
3. Hodgetts S, Radley H, Davies M, Grounds MD. Reduced necrosis of dystrophic muscle by depletion of host neutrophils, or blocking TNFalpha function with Etanercept in mdx mice. *Neuromuscul Disord.* 2006; 16:591–602. [PubMed: 16935507]
4. Messina S, Vita GL, Aguenouz M, et al. Activation of NF-kappaB pathway in Duchenne muscular dystrophy: relation to age. *Acta Myol.* 2011; 30:16–23. [PubMed: 21842588]
5. Vetrone SA, Montecino-Rodriguez E, Kudryashova E, et al. Osteopontin promotes fibrosis in dystrophic mouse muscle by modulating immune cell subsets and intramuscular TGF-beta. *J Clin Invest.* 2009; 119:1583–1594. [PubMed: 19451692]
6. Liu J, Marino MW, Wong G, et al. TNF is a potent anti-inflammatory cytokine in autoimmune-mediated demyelination. *Nat Med.* 1998; 4:78–83. [PubMed: 9427610]

7. Selmaj KW, Raine CS. Experimental autoimmune encephalomyelitis: immunotherapy with anti-tumor necrosis factor antibodies and soluble tumor necrosis factor receptors. *Neurology*. 1995; 45:S44–49. [PubMed: 7783912]
8. Selmaj K, Papierz W, Glabinski A, Kohno T. Prevention of chronic relapsing experimental autoimmune encephalomyelitis by soluble tumor necrosis factor receptor I. *J Neuroimmunol*. 1995; 56:135–141. [PubMed: 7860709]
9. Ruddle NH, Bergman CM, McGrath KM, et al. An antibody to lymphotoxin and tumor necrosis factor prevents transfer of experimental allergic encephalomyelitis. *J Exp Med*. 1990; 172:1193–1200. [PubMed: 2212948]
10. TNF neutralization in MS: results of a randomized, placebo-controlled multicenter study. The Lenercept Multiple Sclerosis Study Group and The University of British Columbia MS/MRI Analysis Group. *Neurology*. 1999; 53:457–465. [PubMed: 10449104]
11. Reinhart K, Karzai W. Anti-tumor necrosis factor therapy in sepsis: update on clinical trials and lessons learned. *Crit Care Med*. 2001; 29:S121–125. [PubMed: 11445746]
12. Spencer MJ, Marino MW, Winckler WM. Altered pathological progression of diaphragm and quadriceps muscle in TNF-deficient, dystrophin-deficient mice. *Neuromuscul Disord*. 2000; 10:612–619. [PubMed: 11053690]
13. Gosselin LE, Barkley JE, Spencer MJ, McCormick KM, Farkas GA. Ventilatory dysfunction in mdx mice: impact of tumor necrosis factor-alpha deletion. *Muscle Nerve*. 2003; 28:336–343. [PubMed: 12929194]
14. Radley HG, Davies MJ, Grounds MD. Reduced muscle necrosis and long-term benefits in dystrophic mdx mice after cV1q (blockade of TNF) treatment. *Neuromuscul Disord*. 2008; 18:227–238. [PubMed: 18207402]
15. Piers AT, Lavin T, Radley-Crabb HG, Bakker AJ, Grounds MD, Pinniger GJ. Blockade of TNF in vivo using cV1q antibody reduces contractile dysfunction of skeletal muscle in response to eccentric exercise in dystrophic mdx and normal mice. *Neuromuscul Disord*. 2011; 21:132–141. [PubMed: 21055937]
16. Pierno S, Nico B, Burdi R, et al. Role of tumour necrosis factor alpha, but not of cyclooxygenase-2-derived eicosanoids, on functional and morphological indices of dystrophic progression in mdx mice: a pharmacological approach. *Neuropathol Appl Neurobiol*. 2007; 33:344–359. [PubMed: 17493014]
17. Chen SE, Gerken E, Zhang Y, et al. Role of TNF- $\alpha$  signaling in regeneration of cardiotoxin-injured muscle. *Am J Physiol Cell Physiol*. 2005; 289:C1179–1187. [PubMed: 16079187]
18. Guttridge DC, Mayo MW, Madrid LV, Wang CY, Baldwin AS Jr. NF-kappaB-induced loss of MyoD messenger RNA: possible role in muscle decay and cachexia. *Science*. 2000; 289:2363–2366. [PubMed: 11009425]
19. Li YP, Schwartz RJ, Waddell ID, Holloway BR, Reid MB. Skeletal muscle myocytes undergo protein loss and reactive oxygen-mediated NF-kappaB activation in response to tumor necrosis factor alpha. *FASEB J*. 1998; 12:871–880. [PubMed: 9657527]
20. Li YP, Reid MB. NF-kappaB mediates the protein loss induced by TNF-alpha in differentiated skeletal muscle myotubes. *Am J Physiol Regul Integr Comp Physiol*. 2000; 279:R1165–1170. [PubMed: 11003979]
21. Jordan MC, Henderson SA, Han T, Fishbein MC, Philipson KD, Roos KP. Myocardial function with reduced expression of the sodium-calcium exchanger. *J Card Fail*. 2010; 16:786–796. [PubMed: 20797603]
22. Li ZB, Kollias HD, Wagner KR. Myostatin directly regulates skeletal muscle fibrosis. *J Biol Chem*. 2008; 283:19371–19378. [PubMed: 18453534]
23. McPherron AC, Lawler AM, Lee SJ. Regulation of skeletal muscle mass in mice by a new TGF-beta superfamily member. *Nature*. 1997; 387:83–90. [PubMed: 9139826]
24. Passier R, Zeng H, Frey N, et al. CaM kinase signaling induces cardiac hypertrophy and activates the MEF2 transcription factor in vivo. *J Clin Invest*. 2000; 105:1395–1406. [PubMed: 10811847]
25. Haq S, Choukroun G, Lim H, et al. Differential activation of signal transduction pathways in human hearts with hypertrophy versus advanced heart failure. *Circulation*. 2001; 103:670–677. [PubMed: 11156878]

26. Yang YJ, Zhu WL, Zhang X, Zhou XW, Zhu ZM. PTEN/PI3K pathways are involved in the signal transduction of myocardial remodeling in patients with congestive heart failure. *Zhonghua Yi Xue Za Zhi*. 2005; 85:1201–1204. [PubMed: 16029597]
27. Toker A, Newton AC. Akt/protein kinase B is regulated by autophosphorylation at the hypothetical PDK-2 site. *J Biol Chem*. 2000; 275:8271–8274. [PubMed: 10722653]
28. Monaco AP, Kunkel LM. Cloning of the Duchenne/Becker muscular dystrophy locus. *Adv Hum Genet*. 1988; 17:61–98. [PubMed: 3055851]
29. Ohlendieck K, Ervasti JM, Snook JB, Campbell KP. Dystrophin-glycoprotein complex is highly enriched in isolated skeletal muscle sarcolemma. *J Cell Biol*. 1991; 112:135–148. [PubMed: 1986002]
30. Ohlendieck K, Campbell KP. Dystrophin-associated proteins are greatly reduced in skeletal muscle from mdx mice. *J Cell Biol*. 1991; 115:1685–1694. [PubMed: 1757468]
31. Villalta SA, Nguyen HX, Deng B, Gotoh T, Tidball JG. Shifts in macrophage phenotypes and macrophage competition for arginine metabolism affect the severity of muscle pathology in muscular dystrophy. *Hum Mol Genet*. 2009; 18:482–496. [PubMed: 18996917]
32. Chen YW, Nagaraju K, Bakay M, et al. Early onset of inflammation and later involvement of TGFbeta in Duchenne muscular dystrophy. *Neurology*. 2005; 65:826–834. [PubMed: 16093456]
33. Chu WM. Tumor necrosis factor. *Cancer Lett*. 2013; 328:222–225. [PubMed: 23085193]
34. Ahn J, Kim J. Mechanisms and consequences of inflammatory signaling in the myocardium. *Current hypertension reports*. 2012; 14:510–516. [PubMed: 22986910]
35. Kast RE. Evidence of a mechanism by which etanercept increased TNF-alpha in multiple myeloma: new insights into the biology of TNF-alpha giving new treatment opportunities--the role of bupropion. *Leukemia research*. 2005; 29:1459–1463. [PubMed: 15964626]
36. Morissette MR, Cook SA, Foo S, et al. Myostatin regulates cardiomyocyte growth through modulation of Akt signaling. *Circ Res*. 2006; 99:15–24. [PubMed: 16763166]
37. Morissette MR, Cook SA, Buranasombati C, Rosenberg MA, Rosenzweig A. Myostatin inhibits IGF-I-induced myotube hypertrophy through Akt. *Am J Physiol Cell Physiol*. 2009; 297:C1124–1132. [PubMed: 19759331]
38. Wagner KR, McPherron AC, Winik N, Lee SJ. Loss of myostatin attenuates severity of muscular dystrophy in mdx mice. *Ann Neurol*. 2002; 52:832–836. [PubMed: 12447939]
39. Barton ER, Morris L, Musaro A, Rosenthal N, Sweeney HL. Muscle-specific expression of insulin-like growth factor I counters muscle decline in mdx mice. *J Cell Biol*. 2002; 157:137–148. [PubMed: 11927606]
40. Kim MH, Kay DI, Rudra RT, et al. Myogenic Akt signaling attenuates muscular degeneration, promotes myofiber regeneration and improves muscle function in dystrophin-deficient mdx mice. *Hum Mol Genet*. 2011; 20:1324–1338. [PubMed: 21245083]



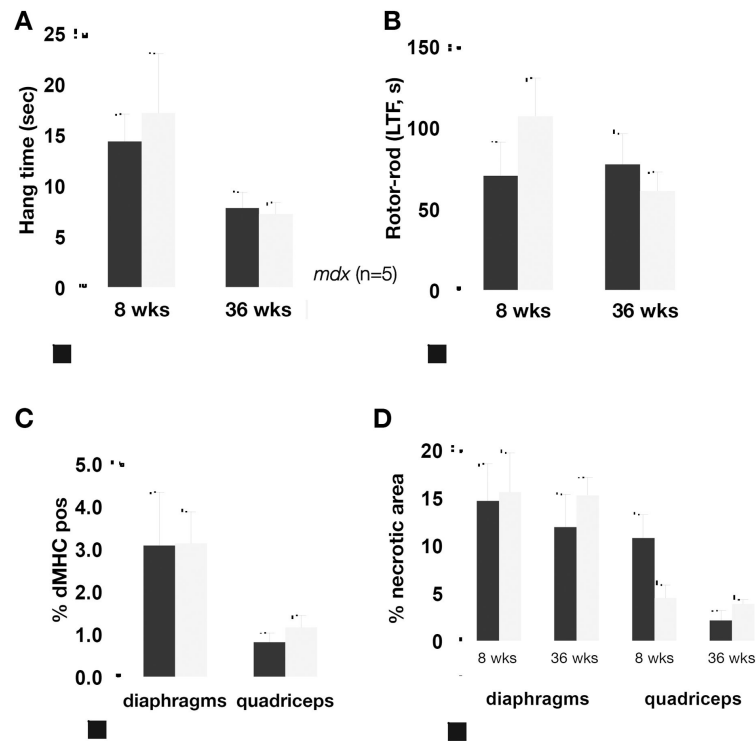


**Figure 1. Short-term treatment with 10 mg/kg Remicade in young and old mice does not produce functional or histological benefits**

(A–B) Functional data of 7 and 38 weeks old *mdx* mice treated once weekly with Remicade beginning at 2 weeks or 28 weeks of age, respectively (Exps 1 and 2, Table 1). The control *mdx* group was injected with non-specific antibody provided by Centocor. Dosage was chosen based on Grounds, 2004 and Hodgetts, 2006. (A) average hang time for wire test in seconds; (B) average latency to fall on Rotor-rod test; (C–D) quantitative histopathology of diaphragm and quadriceps sections to determine; (C) percent regeneration (number of developmental myosin heavy chain positive fibers normalized by total number of fibers) and (D) percent necrosis (assessed after CD11b staining and measurement of all necrotic and pathological areas, normalized by cross sectional area). Vertical bars represent standard error. Statistical significance was assessed by two tailed t-test with significance set at  $p < 0.05$ .

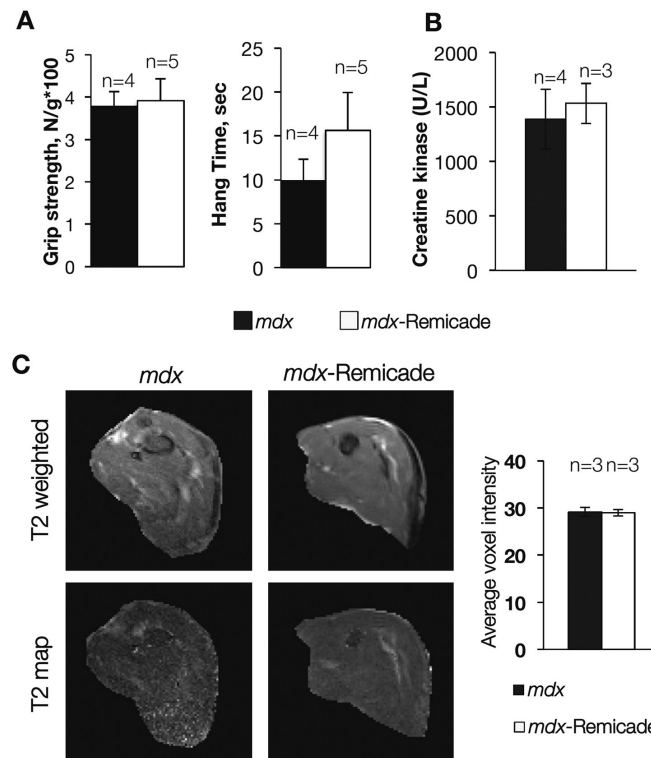


**Figure 2. High dose Remicade (20 mg/kg) treatment of *mdx* mice for 32 weeks does not result in functional or morphological benefits to the *mdx* phenotype**

*Mdx* mice were injected once a week with Remicade (20 mg/kg) or nonspecific control antibody provided by Centocor (20 mg/kg) for 32 weeks, starting at 3 weeks of age. Dosage based on Radley et. al, 2008. (A) Functional data: grip strength (normalized to body weight) and wire test (average hang time in seconds); (B) Serum creatine kinase units/liter; (C) MRI of muscles was carried out at the conclusion of treatment. Shown are representative T2 weighted images and corresponding calculated T2-maps for quadriceps muscles of *mdx* and Remicade treated mice. MRI data are represented as average voxel intensity. Vertical bars represent standard error. No significant differences were observed by two tailed t-test with significance set at  $p < 0.05$ .

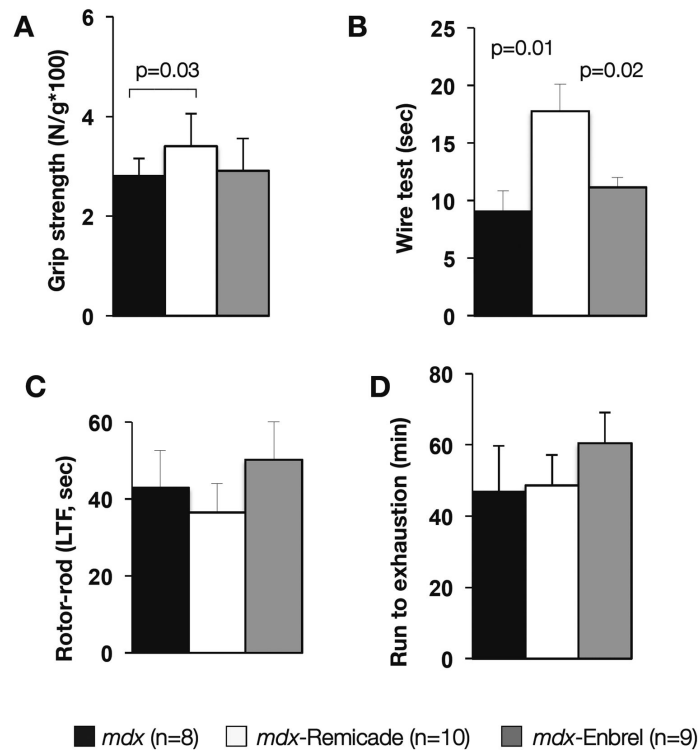


**Figure 3. Remicade dosing at 3 mg/kg improves grip strength and wire test performance**  
 Functional data of *mdx* mice injected with Remicade (3 mg/kg), Enbrel (4 mg/kg) or control (3 mg/kg) once weekly, starting at 6 weeks of age for 24 weeks (Table 1, Exp 4). Enbrel dosing based on Hodgetts, 2006. (A) Grip strength normalized to body weight improved for *mdx* mice treated with Remicade compared to control. No improvement was observed in Enbrel treated mice (B) Average hang-time on the wire improved for Remicade-treated compared to control and Enbrel-treated *mdx* mice. (C) Rotor Rod performance (latency to fall (LTF) was not improved in any group and, neither was (D) the average length of time (minutes) before exhaustion on the treadmill. Vertical bars represent standard error of the mean. Comparisons were made by two tailed t-test with significance set at  $p < 0.05$ .

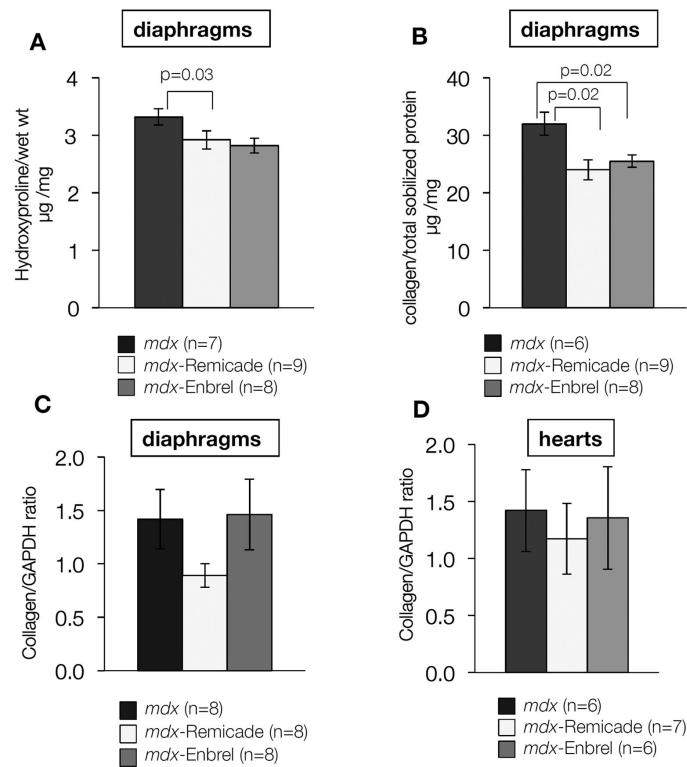


**Figure 4. Prolonged treatment (24 weeks) of *mdx* mice with Remicade (3 mg/kg) or Enbrel (4 mg/kg) decreases fibrosis, as estimated by collagen content**  
 Hydroxyproline (A) and Sircol assays (B) showed significantly less diaphragm collagen content following 24 weeks of TNF blockade with Remicade or Enbrel. (C–D) Levels of Collagen 1a expression assessed by quantitative, real time PCR in the diaphragms (C) and hearts (D) of untreated *mdx* mice compared with Remicade and Enbrel-treated animals. *GAPDH* PCR was used as a cDNA control. Real-time PCR data is shown in graph as average Starting Quantity (SQ) for collagen gene normalized by SQ for *GAPDH*. Vertical bars on all graphs represent standard error. Statistics were assessed by two tailed t-test with significance set at  $p < 0.05$ .

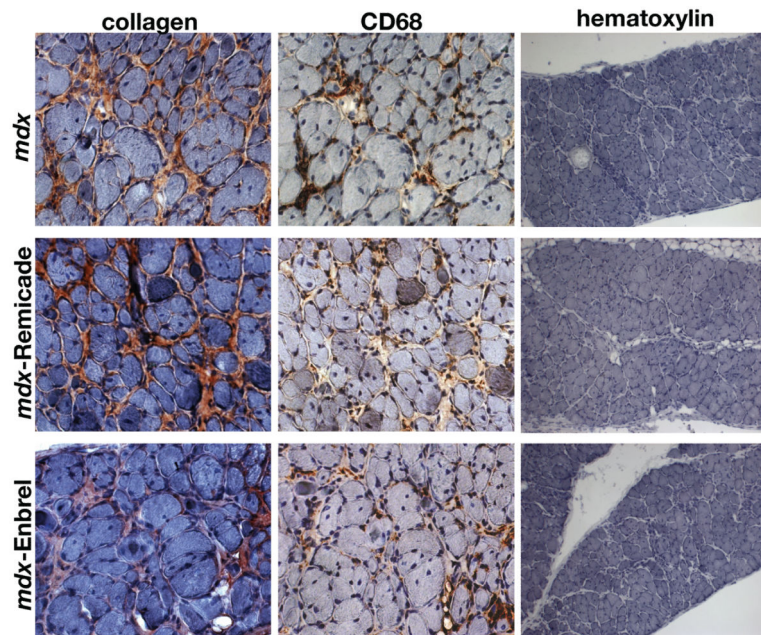


**Figure 5. Morphology of diaphragms from Remicade and Enbrel treated mdx mice**  
Cross sections of diaphragms stained for type I collagen (left) CD68 (macrophage marker, middle) and hematoxylin (right). Staining appears red and sections are counterstained by hematoxylin, which stains cytoplasm light blue and nuclei dark blue. No distinctions between the groups could be made by histological assessment. Animals shown were treated for 24 weeks with Remicade (3 mg/kg) or Enbrel (4 mg/kg) starting at 6 weeks of age. Control group was injected with control antibody provided by Centocor.

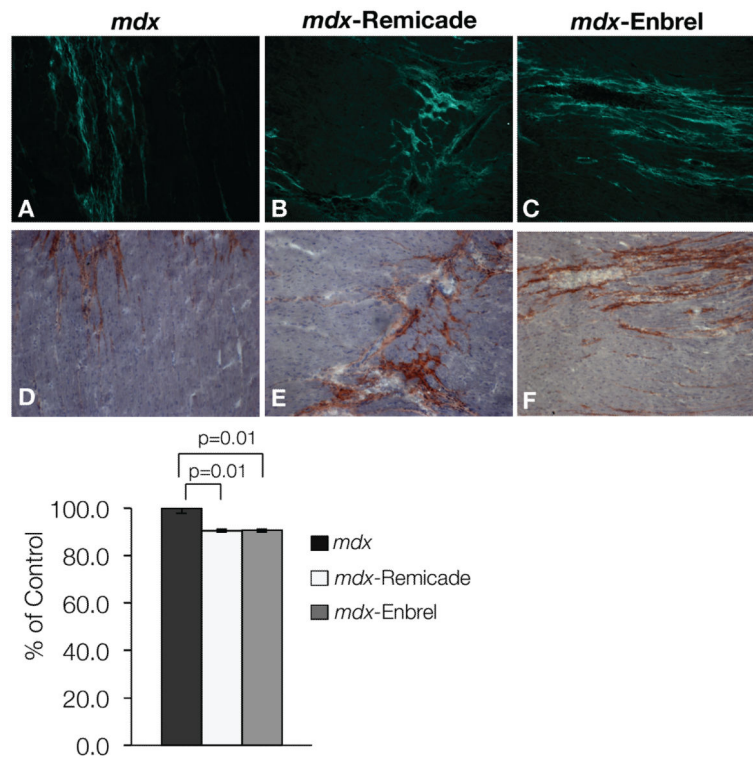


**Figure 6. Reduced collagen content was observed by quantitative histology in the hearts of *mdx* mice treated with Remicade (3 mg/kg) and Enbrel (4 mg/kg) for 24 weeks**  
Collagen content in the hearts of *mdx* mice treated with Remicade and Enbrel was estimated by scanning the entire cross section of slides stained with a specific type I collagen antibody. 4 slides from each heart of 3 *mdx*, 5 Remicade and 4 Enbrel treated animals were analyzed. Values were quantitated using Definiens software and normalized for the cross sectional area. Collagen content in *mdx* mice was set as 100%. Data were analyzed by t-test with  $p<0.05$  considered significantly different.

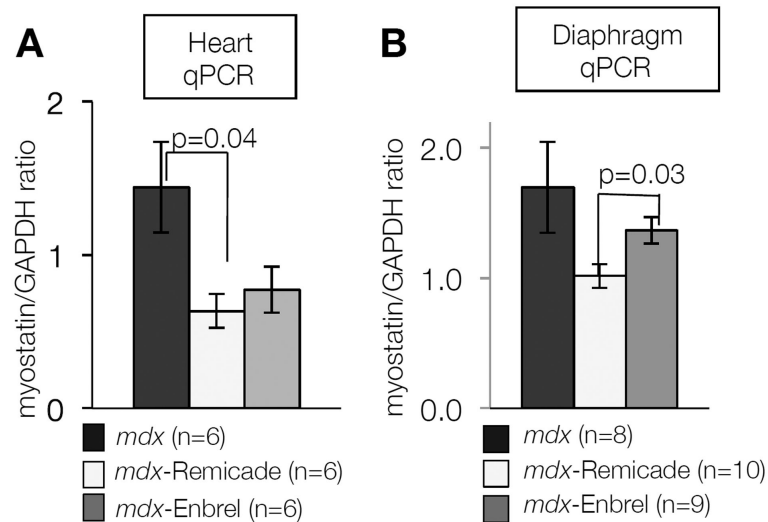


**Figure 7. Decreased myostatin content in *mdx* quadriceps, diaphragms and hearts after 24 weeks of treatment with Remicade (3 mg/kg)**

Levels of myostatin were estimated by quantitative, real time PCR in the hearts (A) and diaphragms (B) of untreated *mdx* mice compared with Remicade and Enbrel-treated animals. Real-time PCR data are shown as average Starting Quantity (SQ) for the gene normalized by SQ for *GAPDH*. Vertical bars on all graphs represent standard error. Statistics were assessed by two tailed t-test with significance set at  $p < 0.05$ .

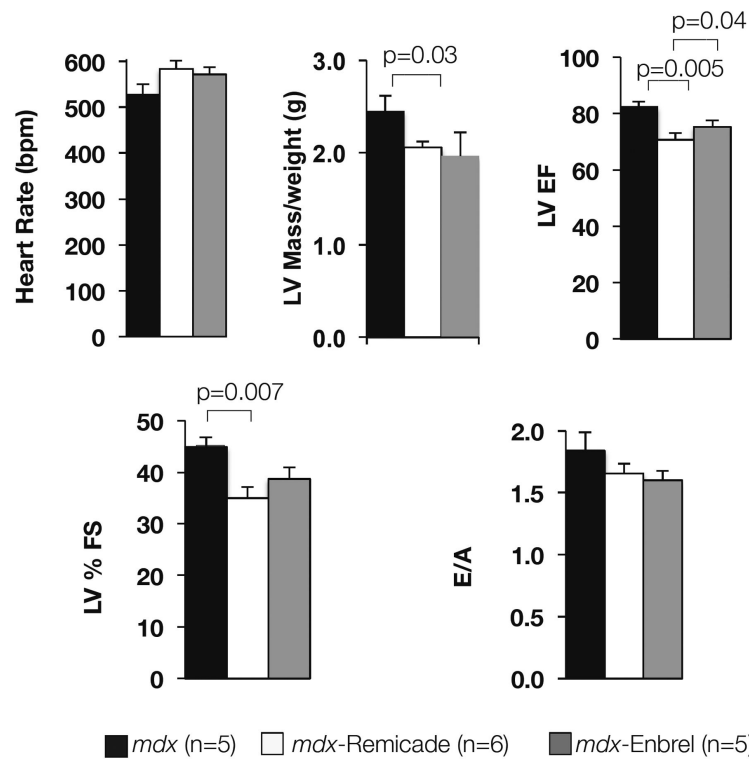


**Figure 8. Echocardiography reveals reduced cardiac function in Remicade treated *mdx* mice** *Mdx* mice treated with Remicade (3mg/kg), Enbrel (4mg/kg) and control (3mg/kg) for 24 weeks were subjected to echocardiography. Left ventricular (LV) mass normalized for body weight, ejection fraction (EF), and fractional shortening (FS) decreased for Remicade treated *mdx* mice. E/A ratio characterizes flow across mitral valve (early [E] wave and atrial [A] wave represent passive filling of the ventricle and active filling with atrial systole correspondingly). Bars represent standard error of mean. Statistics were assessed by two tailed t-test with  $p < 0.05$  considered significantly different.



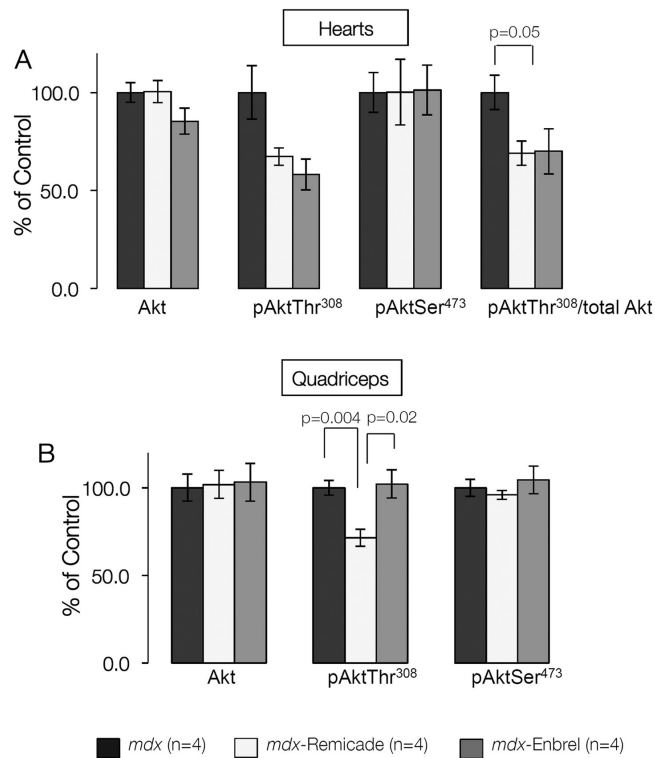


**Figure 9. Reduction in phospho Thr<sup>308</sup>-Akt in *mdx* hearts (A) and quadriceps (B) after 24 weeks of treatment with Remicade (3 mg/kg)**

Levels of Akt and two forms of activated phospho-Akt were assessed by Western blotting in the hearts (A) and quadriceps (B) of untreated *mdx* mice compared with Remicade and Enbrel-treated animals. Akt, pAkt-Thr<sup>308</sup> and pAkt-Ser<sup>473</sup> specific antibodies were utilized to evaluate protein content in heart homogenates prepared in the presence of phosphatase and protease inhibitors. Blots were analyzed by ImageJ software and specific signals were normalized for loading. All values were expressed as percent of average *mdx* normalized signal. Vertical bars on all graphs represent standard error. Statistics were assessed by two tailed t-test with significance set at p=0.05.

**TABLE 1**

## TNF Blockade Injection Protocols

Exp#		Duration (1x/wk)	Treatment Ages	Drug	Dosage (references)
1	<i>Short term young mice</i>	6 weeks	2–8 wks	Remicade	10 mg/kg Grounds, 2004, Hodgetts, 2006
2	<i>Short term old mice</i>	7 weeks	28–36 wks	Remicade	10 mg/kg Grounds, 2004, Hodgetts, 2006
3	<i>Long term young mice high dose</i>	32 weeks	3–36 wks	Remicade	20 mg/kg Radley, 2008
4	<i>Long term young mice low dose</i>	24 weeks	6–30 wks	Remicade Enbrel	3 mg/kg 4 mg/kg Enbrel:Hodgetts, 2006